



Pyrroloquinoline Based Styryl Dyes Doped PMMA, PS, and PS/TiO₂ Polymer for Fluorescent Applications

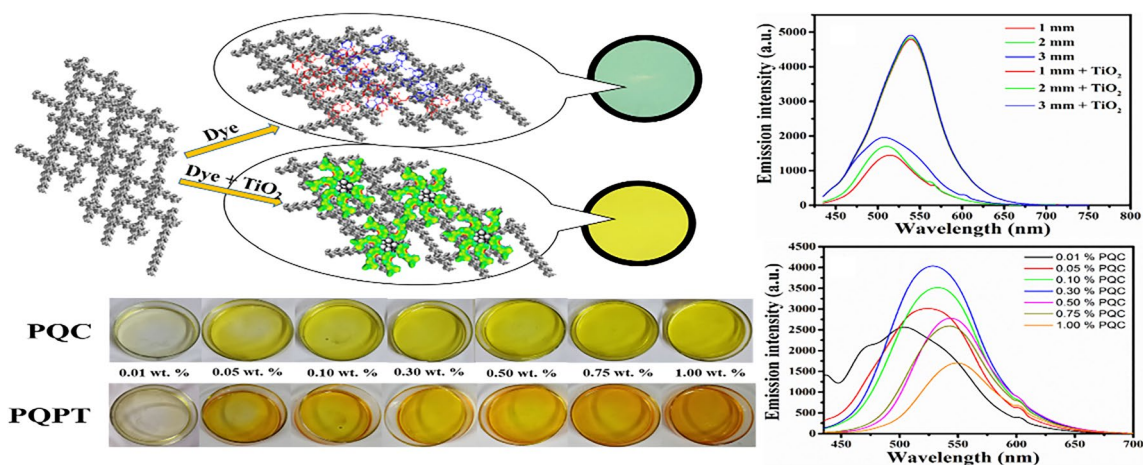
Mahesh Jachak¹ · Rupali Bhise¹ · Ankur Chaturvedi¹ · Vidula Kamble¹ · Ganapati Shankarling¹

Received: 29 November 2021 / Accepted: 7 March 2022 / Published online: 4 April 2022
© The Author(s), under exclusive licence to Springer Science+Business Media, LLC, part of Springer Nature 2022

Abstract

This article presents two highly fluorescent donor- π -acceptor (D- π -A) moieties containing an electron-donating carbazole and phenothiazine donors fused with electron-withdrawing pyrrolo-quinoline acceptor dyes, **PQC** and **PQPT**. We also discussed the polymerization and film-forming process of dye **PQC** and **PQPT** doped in poly (methyl methacrylate) (PMMA) and polystyrene (PS) polymer to find their optical applications in polymer-based technology. We investigated the fluorescent properties of dyes **PQC** and **PQPT** from 0.01 to 1 wt% in poly(methyl methacrylate) (PMMA). We also investigated the changes in the spectrum shape and shift in wavelength with changes in poly(methyl methacrylate) (PMMA), polystyrene (PS), and TiO₂ doped in polystyrene (PS/TiO₂). The analysis of surface morphology of prepared polymer samples was done with the help of a scanning electron microscope. The thermal and photostability of synthesized dyes in poly (methyl methacrylate) (PMMA), polystyrene (PS), and TiO₂ doped in polystyrene (PS/TiO₂) were investigated to get detailed information owing to the application of fluorescent polymers in the field of optoelectronic, nanohybrid coatings in solar concentrators, etc.

Graphical Abstract



Keywords Fluorescent styryl dyes · Poly (methyl methacrylate) · Fluorescence molecular rotors (FMRs) · Polystyrene · Deep eutectic solvent

✉ Ganapati Shankarling
gsshankarling@gmail.com

¹ Department of Speciality Chemicals Technology, Institute of Chemical Technology, N. P. Marg, Matunga, Mumbai, Maharashtra 400019, India

1 Introduction

The poly (methyl methacrylate) (PMMA) is one of the most transparent and durable materials; hence it has been used in many fields and applications such as lenses for glasses [1],

LCD screens [2, 3], medical technologies, and implants [4], solid-state dye lasers [5], signs and artistic uses [6].

The polystyrene (PS) is cheap, transparent, rigid, easy to mould, and has good electrical properties, which open up the application in different fields such as protective packaging [7], automobile parts [8], insulation, and electronics [9], etc.

The multilayer films of biopolymer for controlled release of drug molecules are extensively studied in recent years [10–12]. The addition of small amounts of fluorescent dye in the polymer can make the polymer fluorescent [13]. The temperature responsive copolymer-coated silica nanoparticles for long-term release of fluorescent favipiravir was recently studied [14]. A fluorescent dye-doped in epoxy polymer used to identify cracks and self-healing coating [15–17], transparent biocompatible [18], grafted to glass [19], repair of artifacts [20, 21], solar concentrators [22], and holographic patterning [23]. Also, the dye-doped in PMMA and PS can be used in graded-index polymer optical fiber [24, 25], sensor application [26, 27], solvatochromic dye for humidity measurement [28], solar collector [29, 30], and optical bistability [31].

One of the broadly applicable donor–acceptor type dyes are the styryl dyes which possess improved π -conjugated structures with an increase in intramolecular charge-transfer (ICT) mechanism. The styryl derivatives show high molar absorptivity, good charge transfer characteristics, improved thermal and photostability [32–34]. Also, the metal–organic framework shows improved photoluminescence and chemical stability [35].

By tuning donor, acceptor, and π -conjugation system of a dye, resulted in alter the UV to near-infrared spectra for application in various fields such as optical writing and reading [36], red emitter [37], photonic optical fibre [38], optoelectronic telecommunication [39], electroluminescent materials [40], and photovoltaic [41].

The high photoluminescence and hole-transport properties are enhanced by electron-rich nitrogen and sulfur atoms in carbazole, quinoline, and thiophene derivatives [42]. Also, carbazole, phenothiazine, and pyrroloquinoline heterocyclic aromatic nature make it chemically and thermally stable, creating prominent optical materials [43].

The main aim of this research is to evaluate the effect on fluorescence in poly (methyl methacrylate) (PMMA) and polystyrene (PS) polymers using new pyrroloquinoline as a common acceptor and carbazole or phenothiazine as a donor of two novel dyes (Fig. 1).

Here, we synthesis of **PQC** and **PQPT** dye in a greener way. The UV–vis and fluorescence analysis to determine the modifications in photophysical spectra. We studied the surface morphology and physical strength of polymer samples with the help of a scanning electron microscope and a flexural test. The photostability of the dye-doped polymer was examined by continuous exposer of radiations. The

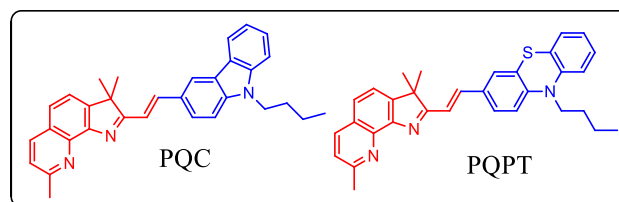


Fig. 1 Structures of synthesized styryl dyes

differential scanning calorimetry (DSC) with thermogravimetry (TGA) is widely studied to explore the thermal properties of the polymers.

2 Experimental Section

2.1 Materials and Instruments

The chemicals and solvents were from Spectrochem Pvt. Ltd., Oxford Lab Fine Chem LLP., and Sigma-Aldrich Ltd. The poly (methyl methacrylate) (PMMA) and polystyrene (PS) polymer was bought from Sigma-Aldrich and used without further purification. Both dyes absorption and fluorescence properties of their respective polymer samples were studied on a Jasco V-750 Uv–vis spectrophotometer and a Jasco FP-8200 spectrofluorometer, respectively. We recorded the differential scanning calorimetric (DSC) and thermogravimetric (TGA) study of dyes and their polymer matrix on a Jasco instrument. The film thickness was measured by the Fizeau interferometer. The tensile strength, and flexural test of polymeric samples, were carried by Instron® modal no. 5566. The study of surface morphology of polymeric samples by using a scanning electron microscope (SEM).

2.2 Experimental Methods

The primary photophysical study of samples was done by using quartz cuvettes of 1 cm path length. The slit width of 5 nm was used to determine the absorbance as well as emission spectra. The experimental conditions were maintained constant in all the experiments. The stock solution of dyes was prepared in chloroform. The dye samples were excited at their higher absorbance wavelength (λ_{max}). The primary photophysical properties of dyes in solution state were carried out in three different solvents with an increase in polarities at a concentration of $\sim 5 \times 10^{-6}$ mol/L. The primary photophysical properties of dyes in poly (methyl methacrylate) (PMMA) was carried out at different concentrations, and the concentration of maximum fluorescence intensity was further used for polystyrene (PS) samples.

2.3 Greener Synthesis Procedure of Styryl Dyes

2.3.1 (E)-2-(2-(9-butyl-9H-carbazol-3-yl)vinyl)-3,3,8-trimethyl-3H-pyrrolo[3,2-h]quinolone (PQC)

In a round bottom flask, added 2 ml of dichloroethane, 2,3,3,8-Tetramethyl-3H-pyrrolo[3,2-h]quinoline (**1**) (1 g, 0.0045 mol) and N-butyl carbazole-4-carbaldehyde (**2**) (1.130 g, 0.0045 mol). Then tetra butyl ammonium bromide (TBAB) (0.160 g, 0.0005 mol) and 5 ml of choline hydroxide were added and heated at 50 °C for 3 h. The completion of the reaction was checked on silica gel TLC with mobile phase (*n*-hexane: ethyl acetate (1:1)). Once the reaction was completed, the removal of dichloroethane was carried on a rotavap and filtered to get solidify the product. The obtained crude product was purified by column chromatography using mobile phase (*n*-hexane: ethyl acetate, (3:2)) to get a yellow-colored solid. Product yield: (1.130 g, 55%), Melting point: 220 °C, ¹H NMR (500 MHz, CDCl₃, TMS) δ 8.35 (s, 1H), 8.16 (d, *J* = 7.7 Hz, 1H), 8.11 (d, *J* = 15.0 Hz, 1H), 8.08 (s, 1H), 7.81 (d, *J* = 8.5 Hz, 1H), 7.67 (d, *J* = 8.0 Hz, 1H), 7.50 (d, *J* = 7.8 Hz, 2H), 7.43 (dd, *J* = 8.2, 3.9 Hz, 2H), 7.36 (d, *J* = 15.0 Hz, 1H), 7.32 (d, *J* = 8.4 Hz, 1H), 7.28 (t, 1H), 4.33 (t, *J* = 7.0 Hz, 2H), 2.88 (s, 3H), 1.87 (m, *J* = 15.1, 7.0 Hz, 2H), 1.60 (s, 6H), 1.42 (m, *J* = 15.1, 7.0 Hz, 2H), 0.96 (t, *J* = 7.0 Hz, 3H).

¹³C NMR (126 MHz, CDCl₃) δ 184.5, 159.9, 147.2, 141.4, 141.1, 140.0, 136.4, 127.6, 127.0, 126.2, 125.4, 125.3, 123.5, 123.0, 122.0, 120.7, 120.4, 119.5, 119.1, 117.8, 109.3, 109.2, 77.2, 53.9, 43.2, 31.3, 25.9, 24.0, 20.7, 14.0, ESI–MS: *m/z* calcd for C₃₂H₃₁N₃ (M⁺): 458.2596, found: 458.2591 [44].

2.3.2 (E)-10-butyl-3-(2-(3,3,8-trimethyl-3H-pyrrolo[3,2-h]quinolin-2-yl)vinyl)-10H-phenothiazine (PQPT)

In a round bottom flask, added 2 ml of dichloroethane, 2,3,3,8-Tetramethyl-3H-pyrrolo[3,2-h]quinoline (**1**) (0.750 gm, 0.00334 mol) and N-butyl phenothiazine 4-carbaldehyde (**3**) (0.947 gm, 0.00334 mol). Then tetra butyl ammonium bromide (TBAB) (0.160 g, 0.0005 mol) and 5 ml of choline hydroxide were added and heated at 40 °C for 6 h. The completion of the reaction was checked on silica gel TLC with mobile phase (*n*-hexane: ethyl acetate (1:1)). Once the reaction was completed, the removal of dichloroethane was carried on a rotavap and filtered to get solidify the product. The obtained crude product was purified by column chromatography using mobile phase (*n*-hexane: ethyl acetate, (3:2)) to get an orange-colored solid. Product yield: (0.979 g, 60%), Melting point: 180 °C, ¹H NMR (500 MHz, CDCl₃, TMS) δ 8.08 (d, *J* = 8.4 Hz, 1H), 7.81 (d, *J* = 15.0 Hz, 1H), 7.67 (d, *J* = 8.0 Hz, 1H), 7.47 (d, *J* = 8.0 Hz, 1H), 7.41 (d,

J = 8.4 Hz, 1H), 7.39 (d, *J* = 1.5 Hz, 1H), 7.31 (d, *J* = 8.4 Hz, 1H), 7.17–7.13 (m, 2H), 7.10 (d, *J* = 15.0 Hz, 1H), 6.92 (t, *J* = 7.5 Hz, 1H), 6.87 (d, *J* = 4.2 Hz, 1H), 6.86 (d, *J* = 4.5 Hz, 1H), 3.88 (t, *J* = 7.5 Hz, 2H), 2.87 (s, 3H), 1.81 (m, *J* = 15.0, 7.5 Hz, 2H), 1.52 (s, 6H), 1.47 (m, *J* = 15.0, 7.5 Hz, 2H), 0.96 (t, *J* = 7.5 Hz, 3H).

¹³C NMR (126 MHz, CDCl₃) δ 184.1, 159.9, 149.1, 147.2, 146.3, 144.6, 141.0, 137.6, 136.5, 130.8, 127.6, 127.5, 127.4, 127.0, 126.1, 125.5, 125.2, 124.2, 122.8, 122.0, 119.1, 118.1, 115.6, 115.5, 77.2, 53.9, 47.5, 29.1, 25.8, 23.6, 20.3, 13.9, ESI–MS: *m/z* calcd for C₃₂H₃₁N₃S (M⁺): 490.2317, found: 490.2310 [44].

3 Results and Discussion

3.1 Design and Synthesis

The synthesized styryl dyes **PQC** and **PQPT** containing the same pyrrolo-quinoline as an acceptor with altered donor units (carbazole for **PQC** and phenothiazine for **PQPT**). The N-butyl aliphatic chain was strategically implemented to reduce the recombination or association of dyes [45]. Here, we synthesis these dyes in an environmentally benign process by using a deep eutectic solvent. The detailed synthesis procedure of intermediates is discussed briefly earlier in the previous paper [44].

Choline hydroxide was prepared by adding choline chloride (2.8 g, 0.01 mol) and potassium hydroxide (1.12 g, 0.01 mol) in 30 ml of methanol and then heated at 60 °C for 12 h. Afterwards, the methanol was removed from rotavap and further used for synthesis without purification [46].

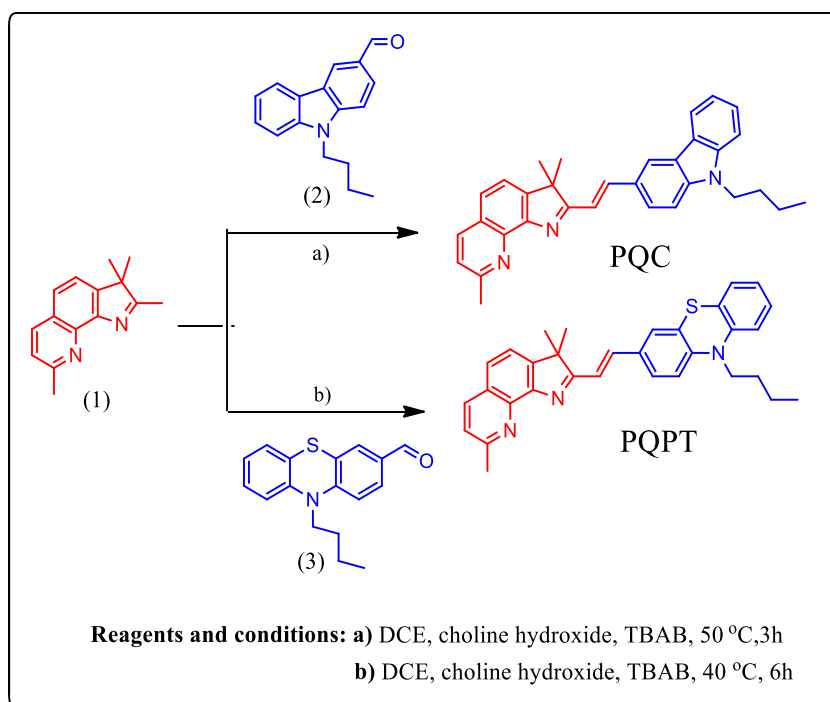
The **PQC** and **PQPT** were synthesized by using Knoevenagel condensation of 2,3,3,8-tetramethyl-3H-pyrrolo[3,2-h]quinoline (**1**) with N-butyl carbazole-4-carbaldehyde (**2**) or N-butyl phenothiazine 4-carbaldehyde (**3**) in dichloroethane with the presence of choline hydroxide and tetra butyl ammonium bromide (TBAB), respectively (Refer Scheme 1).

3.2 Preparation of Fluorescent PMMA Films, PS and PS/TiO₂ Sheets

3.2.1 Preparation of Fluorescent PMMA Films

We added the PMMA grains with **PQC** or **PQPT** fluorescent dyes in dichloromethane (CH₂Cl₂) solvent and sonicated for 1 h at 40 °C. The polymer blend was doped with increased **PQC** or **PQPT** fluorescent dye concentrations from 0.01 to 1 wt%. Further on a clean glass petri dish, the polymer blend was cast and kept dry at room temperature. The fluorescent PMMA films were then aged for 4 h at 55 °C to remove the remaining solvent. The obtained fluorescent films were cut

Scheme 1 Synthetic procedure of dyes **PQC** and **PQPT**



into 4 cm² square portions having 100 ± 10 μm thickness [47]. Figure 2 displays a picture of the **PQC** and **PQPT** dyes fluorescent PMMA films, which shows that the uniformity of dye in the thin film with an increase in the concentration having yellow and orange shades.

3.2.2 Preparation of Fluorescent PS Sheet

The Polystyrene (PS) sheets were prepared using a melt blending process in a Rheomix 3000 blender machine having a volume capacity of 300 cm³, and counter-rotating roller blades were delivered to the kneader having a residence time of 10 min at a mixing speed of 100 rpm. The 0.3 wt% of the synthesized dye **PQC** or **PQPT** and 200 g of Polystyrene (PS) were mixed at 220 °C for 10 min. In an electric-heat curing press, the moulded samples were preheated for 4 min,

having a temperature of 195–200 °C, and then heat pressed. Subsequently, the piece was then conveyed to a cold-pressing instantly and kept for 10 min at 30 °C [48, 49]. The coloured PS samples were moulded into 60 × 40 mm diameter samples thickness of 1 mm, 2 mm, and 3 mm (Fig. 3).

3.2.3 Preparation of PS/TiO₂ Nanohybrid Sheet

The preparation of PS/TiO₂ nanohybrid sheet materials by the same instrument which was used in the fluorescent PS sheet preparation. The 0.3 wt% of the synthesized dye **PQC** or **PQPT**, 0.25 wt% of TiO₂ powder and 200 g of Polystyrene (PS) were mixed at 220 °C for 10 min. The moulded sample was heated for 4 min a having temperature of 195–200 °C and then heat pressed. Subsequently, the piece was conveyed to a cold-pressing instantly and kept

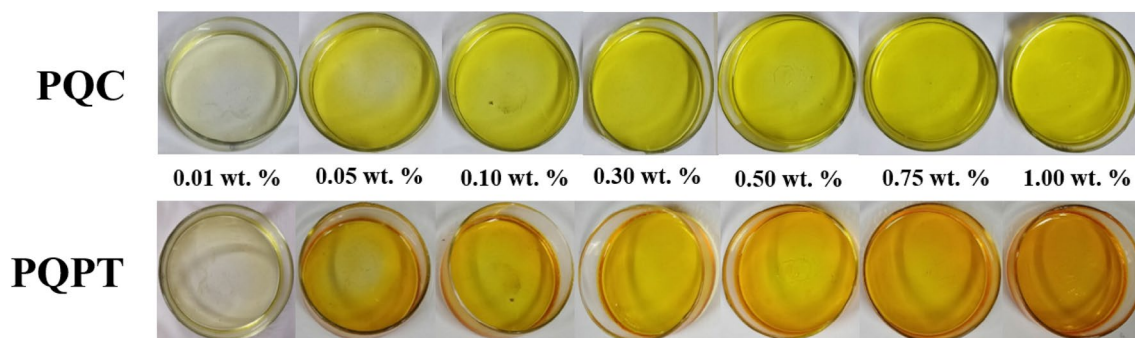


Fig. 2 Cast of increasing concentration of **PQC** and **PQPT** dyes in PMMA films

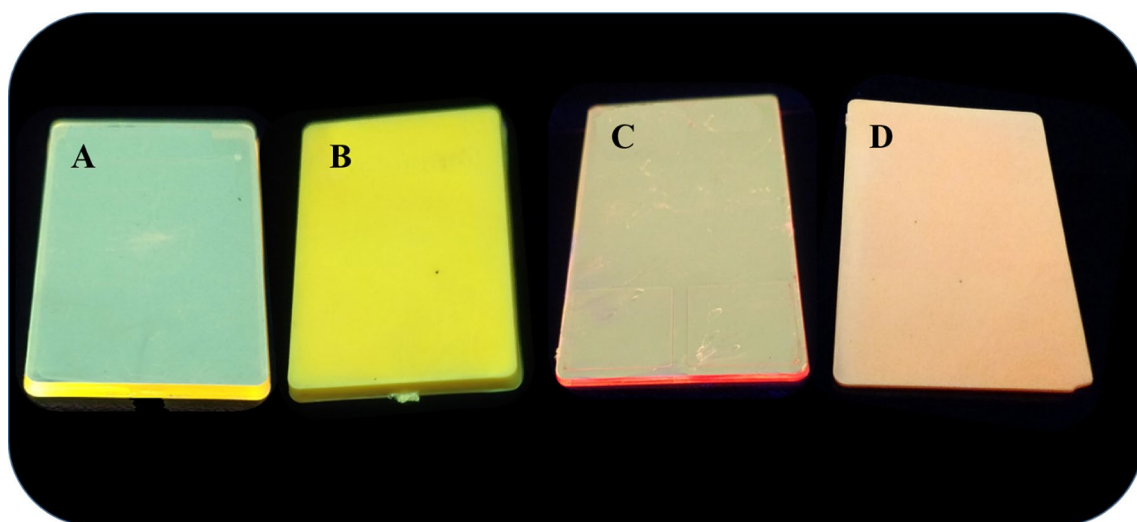


Fig. 3 **A** PQC and **C** PQPT dyes doped in polystyrene polymer without TiO₂ and **B** PQC and **D** PQPT dyes doped in polystyrene polymer with TiO₂ ($c=0.3$ wt% dye-doped)

for 10 min at 30 °C [48, 49]. The coloured PS samples were moulded into 60×40 mm diameter samples having a thickness of 1 mm, 2 mm, and 3 mm (Fig. 3).

3.3 Photophysical Properties

The PQC and PQPT contain the same acceptor but different donor moiety, which results in a change of absorption and emission spectra in the various solvent with an increase in solvent polarity. The difference in photophysical properties causes a shift in the HOMO/LUMO energy bandgap. Therefore, we previously studied the primary photophysical properties of dyes in seven solvents with increased solvent polarity. Their photophysical properties were studied in detail in a previous paper [44]. Here, we shortly discuss the absorption and emission process of PQC and PQPT in three different solvents with the increase in solvent polarities are shown in Fig. 4 and tabulated the calculated photophysical figures in Table 1. The PQC and PQPT show bathochromic shifts from 402 to 405 nm and 423 to 425 nm, respectively, from toluene to methanol. The bathochromic shift in maximum absorption wavelength specifies an increase in intramolecular charge transfer from non-polar to polar solvent. Also, it displays a bathochromic shift in emission spectra such as 487–517 nm for PQC and 545–605 nm for PQPT from non-polar (toluene) to polar (methanol) solvent, which shows that the excited state is more stabilized in the polar solvents as compared to non-polar solvent. The calculated full width at half maximum (FWHM) from absorption peak was 76 nm for PQC as well as 122 nm for PQPT in toluene, which indicates that the existing dye opens up its use in the field of optoelectronics [50]. The obtained

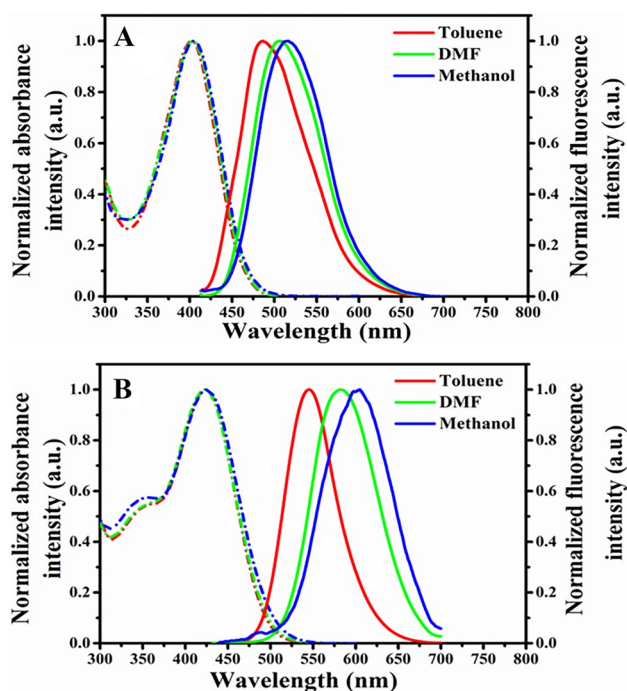


Fig. 4 Absorption and emission spectra of PQC (A), and PQPT (B), in various solvents ($c \sim 5 \times 10^{-6}$ mol/L)

values of Stokes shift for PQC (83–109 nm) and PQPT (119–177 nm) from toluene to methanol. The increase in Stokes shift from non-polar to polar solvent indicates that the emissive state is more stable than the ground state in a molecule.

The quantum yields of dyes were calculated using the help of standard fluorescein ($\phi = 0.79$) in 0.1 mol/L NaOH solution [51] using the following Eq. (1)

Table 1 Experimental photophysical data of **PQC** and **PQPT** in different solvents

Comp	Solvent	λ_{\max}^a (nm)	$\log \epsilon^b$	FWHM ^c (nm)	λ_{onset}^d (nm)	ΔE_{opt}^e (eV)	λ_{exc}^f (nm)	λ_{em}^g (nm)	$\Delta\lambda_s^h$ (nm)	Φ^i
PQC	Toluene	402	4.95	76	461	2.69	404	487	83	0.0782
	DMF	404	4.89	79	464	2.67	406	506	100	0.0144
	Methanol	405	4.92	78	468	2.65	408	517	109	0.0002
PQPT	Toluene	423	4.67	122	491	2.53	426	545	119	0.0922
	DMF	423	4.65	128	493	2.52	425	582	157	0.0208
	Methanol	425	4.56	141	498	2.49	428	605	177	0.0002

^aAbsorption maxima at molar concentration of $c = \sim 5 \times 10^{-6}$ mol/L

^bMolar extinction coefficient calculated from the absorbance at $c = \sim 5 \times 10^{-6}$ mol/L

^cFull width at half maximum (FWHM)

^dOnset absorption edge

^eOptical band gap calculated from the equation, $\Delta E_{\text{opt}} = 1240/\lambda_{\text{onset}}$

^fExcitation maxima

^gEmission maxima at molar concentration of $c = \sim 5 \times 10^{-6}$ mol/L

^hStokes shift

ⁱFluorescence quantum yield calculated using fluorescein as a standard ($\phi = 0.79$ in 0.1 mol/L NaOH.)

$$\Phi_u = \frac{\Phi_{\text{st}} \cdot A_{\text{st}} \cdot F_u \cdot n_u^2}{A_u \cdot F_{\text{st}} \cdot n_{\text{st}}^2} \quad (1)$$

where A_{st} and A_u are the maximum absorbance value of the standard and unknown sample, n_{st} and n_u are the refractive indices of the standard and unknown and solvent, F_{st} and F_u are the areas of the standard and unknown emission spectra, Φ_{st} and Φ_u are the quantum yield of a standard and unknown sample.

In Table 1, the quantum yield in the non-polar (toluene) solution was more relative to the polar (methanol) solution, which signifies the presence of intramolecular charge transfer (ICT) along with twisted intramolecular charge transfer (TICT) in a solvent [52]. The ICT and TICT of these compounds were investigated by using dipole moments and Weller's and Rettig plot. The solvatofluorochromic properties of dyes was investigated by using Lippert–Mataga, E_T (30) and McRae plot. The detailed study of the electron transfer process was investigated briefly earlier in the paper [44].

The molecular rotation of π -bridge in **PQC** and **PQPT** dye in non-viscous solution causes decreases in the fluorescence intensity. As the viscosity of the solution increased, the fluorescence intensity was increased due to the restriction of π -bridge rotation. In the previous paper, we have studied the viscosity study of **PQC** and **PQPT** dyes in the methanol: PEG 400 system, which proves that the fluorescence intensity of dyes increases as the percentage of PEG 400 increases in methanol due to an increase in viscosity of the solution [44]. The attractive results obtained in the viscosity study of dyes make it interesting

to investigate the effect of dye doping in the PMMA, PS, and PS/TiO₂ to open up applications of dyes in the field of polymer.

We studied the photophysical properties of **PQC** and **PQPT** doped in PMMA and Polystyrene polymer to get primary properties information of dyes in these polymers. We discussed above the brief preparation procedure of **PQC** and **PQPT** doped polymer in the PMMA, PS, and PS/TiO₂.

The optical emission spectra of **PQC** and **PQPT** fluorescent dye in PMMA from 0.01 to 1 wt% concentration was shown in Figs. 5 and 6 and tabulated the obtained data in Table 2. The one major band appears related to singlet electronic transfer from $S_0 \rightarrow S_1$ state within the dye [53]. From, the Beer-Lambert law concluded that 0.3 wt% is the optimum dye concentration for **PQC** and **PQPT** with increasing dye concentrations from 0.01 to 1 wt% in the PMMA polymer. Figure 5 shows emission spectra of **PQC** and **PQPT** fluorescent films, which excited at the wavelength to maximum absorption value of 404 nm for **PQC** and 423 nm for **PQPT**. The obtained fluorescence intensity indicates that the dye concentration doped in the polymer is significantly effective in increasing fluorescence intensity up to the dye concentration of 0.3 wt% for **PQC** and **PQPT** dyes. The fluorescence intensity decreases at a maximum dye concentration greater than 0.3 wt% of dye-doped in polymer with spectra broadening. Figure 6 shows the graph of **PQC** and **PQPT**, with a positive slope from dye concentration 0.01 to 0.3 wt% and negative slope from 0.3 to 1 wt%. For **PQC** and **PQPT** dyes doped in PMMA polymer from 0.01 to 1 wt% shows red-shifted in emission spectra from 504 to 549 nm for **PQC** and 539–563 nm for **PQPT**, and full width half maxima (FWHM) of emission wavelength was reduced from

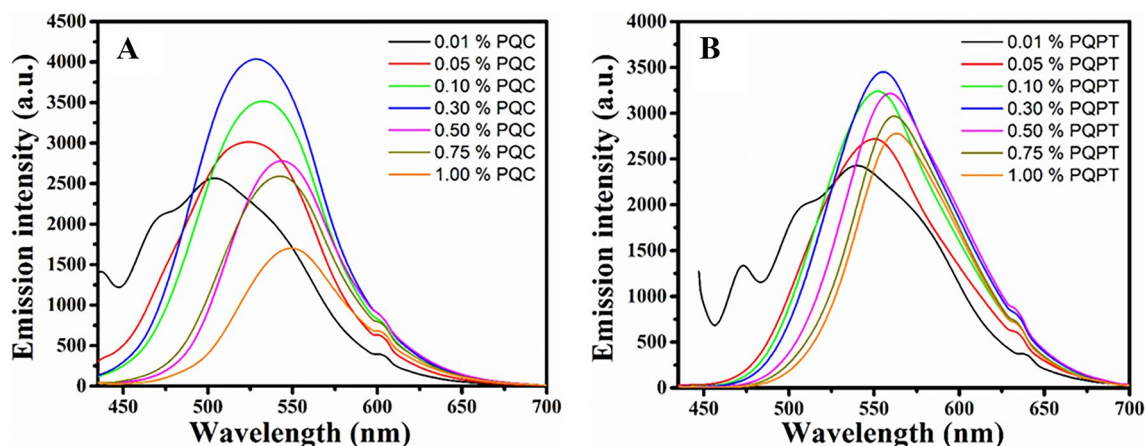


Fig. 5 The fluorescence spectra of **A** PQC and **B** PQPT dye doped in PMMA films

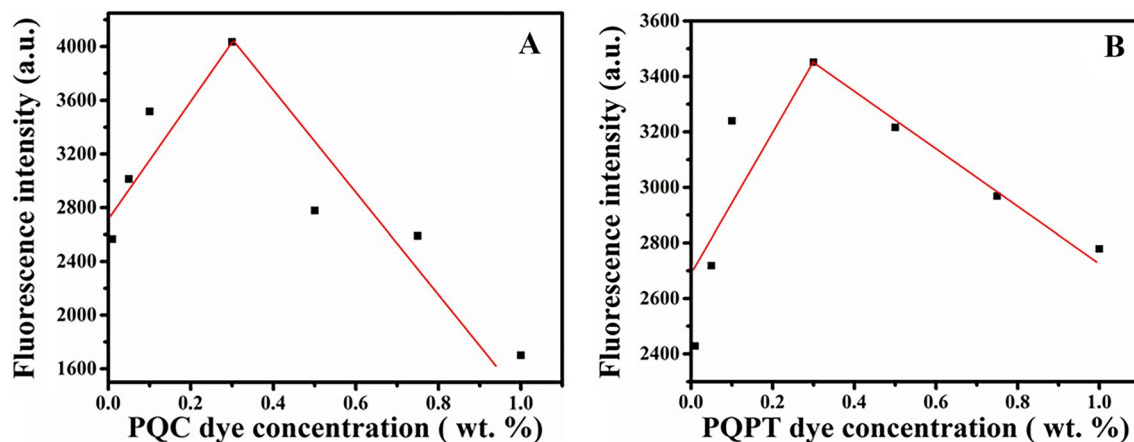


Fig. 6 The fluorescence intensity with increasing in the dye concentration **A** PQC and **B** PQPT

Table 2 Experimental photophysical data of PQC and PQPT dye doped in PMMA with an increase in concentration

Dye doped concentration (wt%)	PQC doped in PMMA		PQPT doped in PMMA	
	$\lambda_{\text{emi}}^{\text{a}}$ (nm)	FWHM ^b (nm)	$\lambda_{\text{emi}}^{\text{a}}$ (nm)	FWHM ^b (nm)
0.01	504	117	539	123
0.05	524	94	551	93
0.10	531	86	553	88
0.30	533	85	556	87
0.50	542	76	559	84
0.75	544	78	562	79
1.00	549	77	563	77

^aEmission maxima

^bFull width at half maximum (FWHM)

117 to 77 nm for PQC, and 123 to 77 nm for PQPT was observed. The tabulated the results in Table 2. The above observation can be clarified based on H and J-aggregate formation. The weak fluorescent intensity in H-aggregate form and decreased fluorescence intensity from dye concentration more than 0.3 wt% in PMMA polymer for both PQC and PQPT dye [54].

The obtained results of PQC and PQPT doped in PMMA polymer show a maximum emission value at 0.3 wt%, which is further used to study the PQC and PQPT dyes in polystyrene polymer.

Yang et al. studied the characterization of nano-TiO₂ doped polystyrene to improve the polystyrene sheet tensile strength and heat resistance [48]. The study shows that 0.25 wt% of TiO₂ doped in polystyrene shows promising results. Hence to improve the photo-stability and efficiency

of polystyrene polymer was studied by doping TiO_2 nano-hybrid with doping of 0.25 wt% of TiO_2 in polystyrene. The 0.3 wt% **PQC** and **PQPT** dye doped in polystyrene polymer were prepared with a thickness of 1 mm, 2 mm, and 3 mm having a doping of TiO_2 and without TiO_2 .

Figure 7 shows the fluorescence spectra of the **PQC** and **PQPT** fluorescent sheet, which excited at its maximum absorption value of 404 nm for **PQC** and 423 nm for **PQPT**. The tabulated obtained data is in Table 3. Both **PQC** and **PQPT** show a blue shift in fluorescence spectra (514 to 507 nm for **PQC** and 541 to 532 nm for **PQPT**) with the increase in fluorescence intensity for polymer thickness 1 mm to 3 mm in the absence of TiO_2 doping. The polystyrene polymer thickness of 1 mm containing **PQC** or **PQPT** dye-doped with TiO_2 shows a remarkable increase in fluorescence intensity of 3.31 fold for **PQC** and 2.76 fold for **PQPT** as compared to polystyrene polymer containing **PQC** or **PQPT** dye-doped without TiO_2 . As

the polymer thickness increases from 1 to 3 mm for TiO_2 doped polymers, not showing a significant increase in fluorescent intensity and emission wavelength was observed for both **PQC** and **PQPT** dye. Also, there was no significant increase in full width at half maxima (FWHM) of emission wavelength observed for **PQC** and **PQPT** dye doped in polystyrene with the absence and presence of TiO_2 . The tabulated the results in Table 3.

3.4 Surface Morphology

The highly soluble pyrrolo-quinaldine based dyes **PQC** and **PQPT** in dichloromethane solvent have a 1 wt% dye allowing the uniform formation of PMMA thin film by solution casting process was analyzed by scanning electron microscope (SEM). The thin PMMA film of **PQC** dye shows smooth and without cracks surface. The SEM image of pure

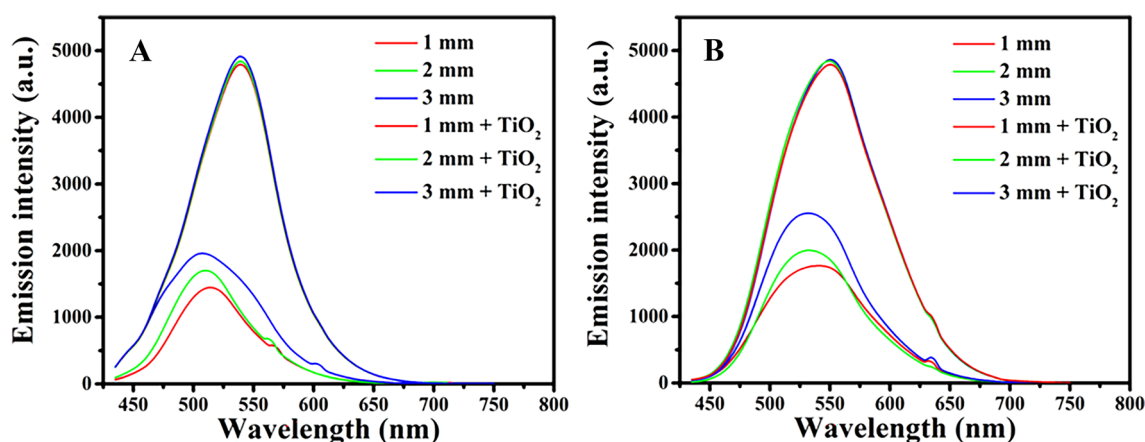


Fig. 7 The fluorescence spectra of **A PQC** and **B PQPT** dye doped in polystyrene sheets of thickness 1 mm to 3 mm ($c=0.3$ wt% dye-doped)

Table 3 Experimental photophysical data of **PQC** and **PQPT** in dye-doped in PS with and without TiO_2

Sheet Thickness (cm)	PQC doped in PS		PQC doped in PS/ TiO_2		PQPT doped in PS		PQPT doped in PS/ TiO_2	
	λ_{em}^a (nm)	FWHM ^b (nm)	λ_{em}^a (nm)	FWHM ^b (nm)	λ_{em}^a (nm)	FWHM ^b (nm)	λ_{em}^a (nm)	FWHM ^b (nm)
0.1	514	79	539	87	542	101	551	101
0.2	510	82	539	87	534	91	550	102
0.3	508	97	539	87	532	90	550	102

^aEmission maxima($c=0.3$ wt% dye doped)

^bFull width at half maximum (FWHM)

PMMA thin film (A), fabricated by solution casting process, shows the same surface morphology as PMMA + 1 wt% PQC dye thin film (B) with no significant large aggregation formation of dyes molecules in thin-film (B), from which we can conclude that a homogeneous distribution of PQC dye in film formation (Fig. 8). The film surface contains very tiny small crater-like structures with a flat bottom in both the samples, which may form during the solvent evaporation process.

The prepared polystyrene (PS) sheets of 3 mm thickness have a 0.3 wt% of PQC dye-doped with 0.25 wt% of TiO₂ or without TiO₂ using a melt blending process examined under SEM image. The SEM image of pure PS (A), PS + 0.3 wt% of PQC dye (B) and PS + 0.3 wt% of PQC dye + 0.25 wt% of TiO₂ (C) shows a uniform distribution of dye in the polymer. The comparison of polystyrene (PS) polymer with PQC dye doped in without TiO₂ (B) and with TiO₂ (C) detected homogenous distribution of TiO₂ in polymer and no significant change in the morphology of the infused TiO₂ (Fig. 9).

3.5 Tensile Strength and Flexural Test

The dye-doped in PMMA, PS and PS + TiO₂ polymers show application in various fields, which may experience different bend and tensile forces during its working. Therefore

it is vital to study the physical strength of dye-doped polymers. The Tensile strength of very flexible thin film of pure PMMA and PMMA + 1 wt% of PQC dye and the flexural test of PS + 0.3 wt% of PQC dye with 0.25 wt% of TiO₂ and without TiO₂ polymer at three-point bending test was calculated by a computer-operated universal machine. We carried out the tensile strength of the polymer sample with a pure PMMA and PMMA + PQC dye on sample length of 20 mm, a width of 7 mm and 100 ± 10 μm thickness. In contrast, a flexural test of PS + PQC dye with and without TiO₂ polymer was carried on sample length of 5 cm, the width of 3.5 cm and thickness of 3 mm having applied traverse speed of 10 mm/min, respectively.

The polymer samples of pure PMMA and PMMA with PQC dye show maximum tensile strength of 2.2 MPa and 2.0 MPa, respectively, which shows that the addition of PQC dye in PMMA polymer has much less effect on the decrease in tensile strength than the pure PMMA polymer.

The PS + PQC dye with and without TiO₂ polymer show a maximum flexural test value of 45.7 kg and 50.7 kg, respectively, which shows that a 10% decrease in flexural strength with the addition of TiO₂ in PS as compared to without TiO₂ added polymer.

Fig. 8 SEM images of **A** Only PMMA, **B** PMMA + 1 wt% PQC Dye

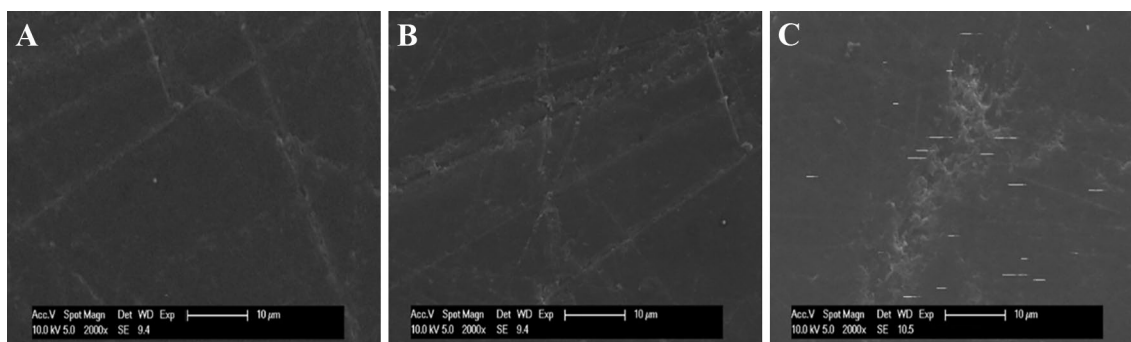
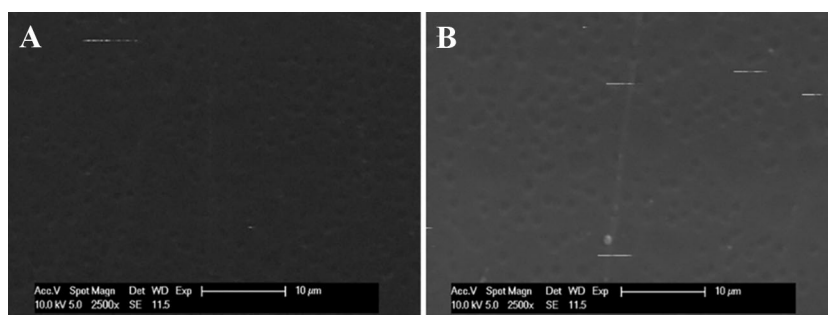


Fig. 9 SEM images of **A** Only PS, **B** PS + 0.3 wt% of PQC dye, and **C** PS + 0.3 wt% of PQC dye + 0.25 wt% of TiO₂

3.6 Photo-Stability

It is an essential parameter for styryl fluorescent dyes to improve their photo-stability, as they show poor photostability under continued radiation in the presence of oxygen. It is necessary to have a significant photostability of styryl fluorescent dyes when its application is in the field of photonics and optoelectronic devices, and laser.

The molecular structures and different substitutes of the dyes influence the photostability of styryl dyes. Therefore we used a 500 W iodine-tungsten (I/W) lamp (working wavelength range = 320–1100 nm) for accelerated photostability measurement by continuously exposing the samples. The experimental samples were exposed to irradiation for 36 h at 28 °C, which corresponds to one year's exposure to the radiation of the terrestrial solar spectrum [55, 56]. The photostability study of **PQC** and **PQPT** was carried out in the same experimental conditions and presented the obtained practical result in Fig. 10.

From Fig. 10, it was concluded that the fluorescence intensity at their respective excited maximum absorption wavelength of **PQC** and **PQPT** dye sample doped in polystyrene without TiO_2 with sample concentration of 0.3 wt% of 1 mm thickness was reduced by 2.85% and 3.06%, respectively, to its **PQC** and **PQPT** dye sample doped in polystyrene with TiO_2 having a concentration of 0.3 wt% and 1 mm thickness under the monitored conditions. A similar trend was observed with 2 mm and 3 mm thickness polymer samples. The photostability study on both the dyes shows that the sample doped with TiO_2 was more stable than the sample without TiO_2 after 36 h of irradiation.

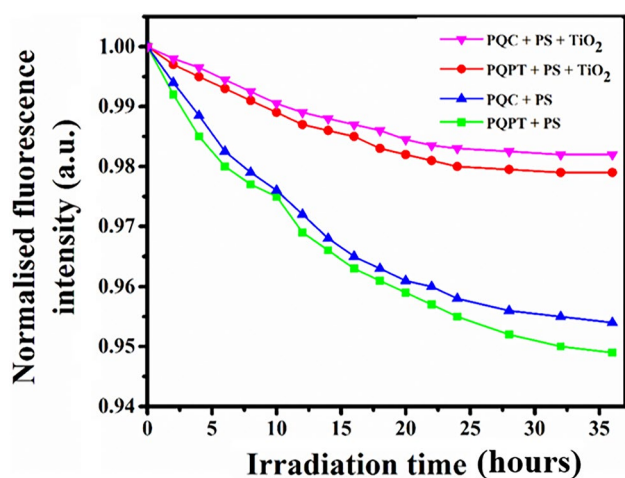


Fig. 10 Accelerated photo-degradation curves of **PQC** and **PQPT** dyes doped in PS sheet with and without TiO_2

Figure 10 shows that **PQC** has more photostability than **PQPT**, which may be due to the improved μ -conjugated structure and influence of phenothiazine donor, which reduces the stability of **PQPT** dye [44]. The above experiment concluded that the addition of TiO_2 on the polystyrene polymer with **PQC** and **PQPT** dye improves photo-stability.

3.7 Thermal Stability

The differential scanning calorimetry (DSC) and thermogravimetric analysis (TGA) were used to study the changes in physical properties of PMMA, polystyrene, and polystyrene doped TiO_2 with the addition of 0.3 wt% of **PQC** and **PQPT** dyes regarding temperature from 30 to 600 °C in the presence of nitrogen atmosphere to 20 °C/minute rise in temperature. From Fig. 11, the thermogravimetric study shows the minimum value of percentage weight loss in dyes under the temperature of 180 °C. The dyes **PQC** and **PQPT** display thermal decomposition temperature (T_d) at 253 °C with a 2.0% reduction in total weight and at 180 °C with a 3.0% reduction in total weight. The above experiment concluded that dyes are thermally stable up to 180 °C. The PMMA polymer showed thermal decomposition temperature (T_d) at 160 °C by a 2.2% reduction in total weight. As the addition of 0.3 wt% of **PQC** and **PQPT** dyes in PMMA polymer showed thermal decomposition temperature (T_d) on 179 °C by 2.0% reduction in total weight and 177 °C with a 2.0% reduction in total weight respectively, which shows that addition of 0.3 wt% of **PQC** and **PQPT** dyes in PMMA polymer does not show more variation in thermal decomposition temperature (T_d) of PMMA polymer (Table 4).

The PS polymer lost 2% mass upon heating to 334 °C (Fig. 11). Upon addition of 0.3 wt% of **PQC** and **PQPT** dyes in PS polymer, the lost 2% mass upon heating to 333–338 °C, which shows no significant weight loss due to the addition of 0.3 wt% of **PQC** and **PQPT** dyes in PS polymer. By adding TiO_2 in polystyrene polymer with 0.3 wt% of **PQC** and **PQPT** dyes shows lost 2% mass upon heating to 362 °C, from which it shows that the addition of TiO_2 in PS polymer increases its thermal properties [57] (Table 4).

Figure 12 represents the DSC analysis of polymers. The endothermic peak observed for **PQC** and **PQPT** at 220 °C and 180 °C shows transition temperature for these dyes, respectively [58]. Figure 12 depicts that there was no significant change observed due to the addition of 0.3 wt% **PQC** and **PQPT** dyes in PMMA and PS polymer. The addition of TiO_2 in 0.3 wt% **PQC** and **PQPT** dyes in PS polymer show the shift of decomposition temperature from 428 to 439 °C for **PQC** and 434 °C to 440 °C for **PQPT**, which signifies that the addition of TiO_2 in 0.3 wt% **PQC** and **PQPT** dyes in PS increase the decomposition temperature.

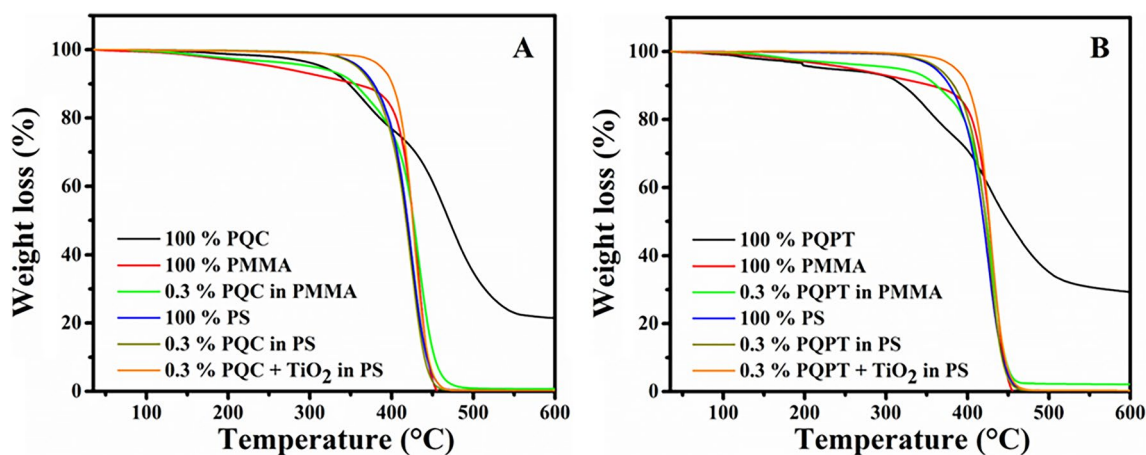


Fig. 11 Thermogravimetric analysis (TGA) of A PQC and B PQPT dye doped in PMMA, PS and PS/TiO₂

Table 4 Experimental thermogravimetric data of PQC and PQPT in dye-doped in PMMA, PS with and without TiO₂

Sample	PQC		PQPT	
	Thermal decomposition temperature	% Weight loss	Thermal decomposition temperature	% Weight loss
Pure dye	253 °C	2.0%	180 °C	3.0%
Pure PMMA	160 °C*	2.2%*	160 °C*	2.2%*
0.3 wt% dye in PMMA	179 °C	2.0%	177 °C	2.0%
Pure PS	334 °C*	2.0%*	334 °C*	2.0%*
0.3 wt% dye in PS	333 °C	2.0%	338 °C	2.0%
0.3 wt% dye in PS + 0.25 wt% of TiO ₂	362 °C	2.0%	362 °C	2.0%

*In the absence of dye

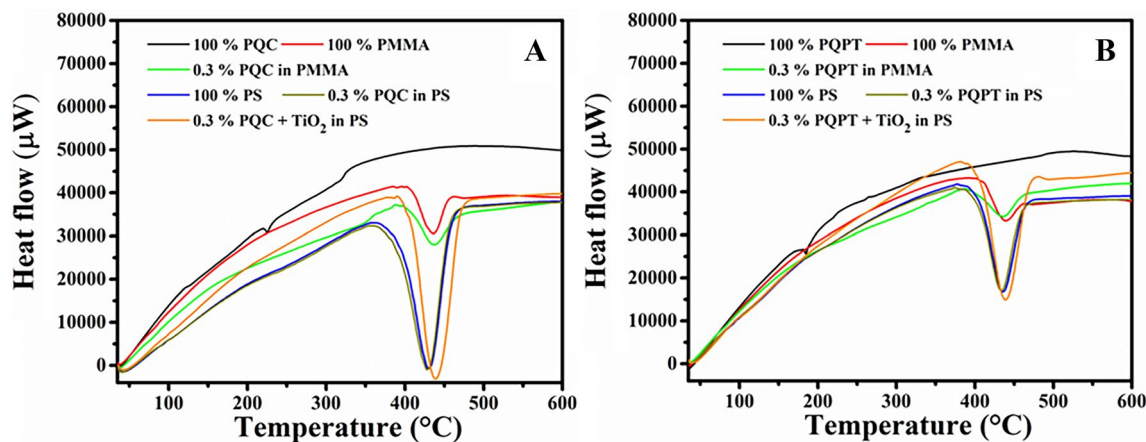


Fig. 12 Differential scanning calorimetric analysis (DSC) of A PQC and B PQPT dye doped in PMMA, PS and PS/TiO₂

4 Conclusions

In this article, novel fluorescent dyes containing pyrroloquinoline acceptor fused with donor carbazole and phenothiazine moiety, **PQC** and **PQPT** doped in the polymeric matrix, was prepared to obtain yellow and orange light emission in the poly(methyl methacrylate) and polystyrene films. The dye concentrations were optimized for better optical limiting performance doped in a polymer. The most promising dye concentration (0.3 wt%) for both the dye was concluded on the background of better photophysical properties to obtain the maximum fluorescence intensity and stability of the polymeric matrix. The bathochromic shift was observed as the dye wt% in PMMA polymer increased. The dye **PQC** and **PQPT** show emission at a wavelength of 528 nm and 555 nm respectively in PMMA polymer at the 0.3 wt% ideal dye concentration in the polymer. The dye **PQC** and **PQPT** demonstrate good solubility and compatibility with PMMA and PS polymer.

The scanning electron microscope shows uniform and homogenous surface morphology of studied polymer samples. As well, the nanohybrid PS/TiO₂ polymer is promising to improve the photo-stability and thermal stability of **PQC**, and **PQPT** fluorescent dye was observed with enhancement in fluorescence properties of dyes, but 10% reduced in the flexural strength of TiO₂ doped polymer was observed. In addition, the improve greener way synthesis procedure of dyes, optical properties and ease of fabrication process, leading to increasing interest of these dyes in optical devices.

We believe that the existing research work will create more interest in researchers to carry out a more study of these dyes for applications in the field of polymer.

Acknowledgements The authors are thankful to UGC-CAS, TEQIP-III for financial support. The instrumental grant from DST-FIST-2018 (Grant section number – SR/FST/ET 582 I/2018/156(C) DATED 24/10/2019). The author's acknowledgement Colourtex Industries Pvt. Ltd. for polystyrene samples preparation.

Funding Funding were provided by UGC-CAS, TEQIP-III and DST-FIST-2018.

Declarations

Competing interest The authors have not disclosed any competing interests.

References

1. M. Curtis, G. Watters, 25—cosmetic and prosthetic contact lenses, in *Speedwell LBT-CL*, ed. by A.J. Phillips (Elsevier, London, 2019), pp. 463–476. <https://doi.org/10.1016/B978-0-7020-7168-3.00025-8>
2. A.R. Prado, A.G. Leal-Junior, C. Marques, S. Leite, G.L. de Sena, L.C. Machado et al., Polymethyl methacrylate (PMMA) recycling for the production of optical fiber sensor systems. *Opt Express* **25**, 30051–30060 (2017). <https://doi.org/10.1364/OE.25.030051>
3. H.M. Abomostafa, D.E. Abulyazied, Linear and nonlinear optical response of nickel core-shell @ Silica/PMMA nanocomposite film for flexible optoelectronic applications. *J Inorg Organomet Polym* **31**, 2902–2914 (2021). <https://doi.org/10.1007/s10904-021-01883-9>
4. S.J. Kim, B. Choi, K.S. Kim, W.J. Bae, S.H. Hong, J.Y. Lee et al., The potential role of polymethyl methacrylate as a new packaging material for the implantable medical device in the bladder. *Biomed Res Int* (2015). <https://doi.org/10.1155/2015/852456>
5. Y.G. Jiang, R.W. Fan, H. Peng, Y.Q. Xia, D.Y. Chen, Tunable solid-state lasers based on PMMA doped with pyromethene dyes. *Laser Phys Lett* **6**, 212–215 (2009). <https://doi.org/10.1002/lapl.200810125>
6. A. Hashim, B. Abbas, Recent review on poly-methyl methacrylate (PMMA)-polystyrene (PS) blend doped with nanoparticles for modern applications. *Res. J. Agric. Biol. Sci.* **14**, 6–12 (2019)
7. M. Niaounakis, 3—polymers used in flexible packaging, in *Niaounakis MBT-R of FPP*, ed. Plast. Des. Libr. (William Andrew Publishing, 2020), pp. 57–96. <https://doi.org/10.1016/B978-0-12-816335-1.00003-7>
8. S.A. Begum, A.V. Rane, K. Kanny, Chapter 20—applications of compatibilized polymer blends in automobile industry, in *Thomas SBT-C of PB*, ed. A.R. A. (Elsevier, 2020), pp. 563–593. <https://doi.org/10.1016/B978-0-12-816006-0.00020-7>
9. R. Mujal-Rosas, X. Ramis-Juan, Electrical application of polystyrene (PS) reinforced with old tire rubber (GTR): dielectric, thermal, and mechanical properties. *Sci Eng Compos Mater* **20**, 233–244 (2013). <https://doi.org/10.1515/secm-2012-0131>
10. Xu. Li, H. Wang, Z. Chu, L. Cai, H. Shi, C. Zhu, D. Pan, J. Pan, X. Fei, Y. Lei et al., Temperature-responsive multilayer films of micelle-based composites for controlled release of a third-generation EGFR inhibitor. *ACS Appl. Polym. Mater.* **2**(2), 741–750 (2020). <https://doi.org/10.1021/acsapm.9b01051>
11. Xu. Li, Z. Chu, H. Wang, L. Cai, Tu. Zhigang, H. Liu, C. Zhu, H. Shi, D. Pan, J. Pan, X. Fei et al., Electrostatically assembled multilayered films of biopolymer enhanced nanocapsules for on-demand drug release. *ACS Appl. Bio Mater.* **2**(8), 3429–3438 (2019). <https://doi.org/10.1021/acsabm.9b00381>
12. A.S.A. Raboh, M.S. El-khooly, M.Y. Hassaan, Bioactivity and drug release study of dexamethasone loaded bioglass/Chitosan composites for biomedical applications. *J. Inorg. Organomet. Polym.* **31**, 2779–2790 (2021). <https://doi.org/10.1007/s10904-021-01936-z>
13. R. Anbarasan, B. Meenarathi, V. Parthasarathy, Structural and thermal studies of fluorescein and Rhodamin6G grafted diblock copolymers. *J. Inorg. Organomet. Polym.* **31**, 3549–3561 (2021). <https://doi.org/10.1007/s10904-021-01978-3>
14. Xu. Li, X. Zhang, Z. Chu, H. Wang, Y. Li, X. Shen, L. Cai, H. Shi, C. Zhu, J. Pan, D. Pan, Temperature-responsive multilayer films based on block copolymer-coated silica nanoparticles for long-term release of favipiravir. *ACS Appl. Nano Mater.* **4**(12), 14014–14025 (2021). <https://doi.org/10.1021/acsnm.1c03334>
15. Y.K. Song, B. Kim, T.H. Lee, S.Y. Kim, J.C. Kim, S.M. Noh et al., Monitoring fluorescence colors to separately identify cracks and healed cracks in microcapsule-containing self-healing coating. *Sens. Actuators B Chem.* **257**, 1001–1008 (2018). <https://doi.org/10.1016/j.snb.2017.11.019>
16. Y.K. Song, T. Lee, J.C. Kim, K. Lee, S. Lee, S. Noh et al., Dual monitoring of cracking and healing in self-healing coatings using microcapsules loaded with two fluorescent dyes

- molecules. *Molecules* (2019). <https://doi.org/10.20944/preprints201904.0035.v1>
17. P. Bolimowski, I. Bond, D. Wass, Robust synthesis of epoxy resin-filled microcapsules for application to self-healing materials. *Philos. Trans. R. Soc. A Math. Phys. Eng. Sci.* **374**, 20150083 (2016). <https://doi.org/10.1098/rsta.2015.0083>
 18. B. De, M. Kumar, B.B. Mandal, N. Karak, An in situ prepared photo-luminescent transparent biocompatible hyperbranched epoxy/carbon dot nanocomposite. *RSC Adv.* **5**, 74692–74704 (2015). <https://doi.org/10.1039/C5RA12131K>
 19. J. Dunkers, J. Lenahrt, J. Van, R. Parnas, Interfacial response of a fluorescent dye grafted to glass. *Langmuir* **16**, 8145–8152 (2000)
 20. W. Yao, M. Tebyetekerwa, X. Bian, W. Li, S. Yang, M. Zhu et al., Materials interaction in aggregation-induced emission (AIE)-based fluorescent resin for smart coatings. *J. Mater. Chem. C* **6**, 12849–12857 (2018). <https://doi.org/10.1039/C8TC04175J>
 21. P.D. McFadden, K. Frederick, L.A. Argüello, Y. Zhang, P. Vandiver, N. Odegaard et al., UV fluorescent epoxy adhesives from noncovalent and covalent incorporation of coumarin dyes. *ACS Appl. Mater. Interfaces* **9**, 10061–10068 (2017). <https://doi.org/10.1021/acsami.6b13218>
 22. A. Partanen, A. Harju, J. Mutanen, H. Lajunen, T. Pakkanen, M. Kuittinen, Luminescent optical epoxies for solar concentrators. *Proc. SPIE* (2014). <https://doi.org/10.1117/12.2061721>
 23. J. Kim, H. Oh, J. Yoo, E. Kim, Fluorescent photopolymer for holographic patterning. *Mol. Cryst. Liq. Cryst.* **491**, 67–73 (2008). <https://doi.org/10.1080/15421400802328956>
 24. M. Kailasnath, T.S. Sreejaya, R. Kumar, C.P.G. Vallabhan, V.P.N. Nampoori, P. Radhakrishnan, Fluorescence characterization and gain studies on a dye-doped graded index polymer optical-fiber preform. *Opt. Laser Technol.* **40**, 687–691 (2008). <https://doi.org/10.1016/j.optlastec.2007.10.015>
 25. Y. Kawabe, K. Fukuzawa, T. Uemura, K. Matsuura, T. Yoshikawa, J. Nishide et al., Formation of photo-induced index grating in azo-carbazole dye-doped polymer. *Proc. SPIE* (2012). <https://doi.org/10.1117/12.928554>
 26. R. Ahmed, Optical properties of rhodamine—B dye doped in transparent polymers for sensor application. *Chin. J. Phys.* **51**, 570 (2013). <https://doi.org/10.6122/CJP.51.570>
 27. M.S. Hamdy, S. AlFaify, A. Al-Hajry, I.S. Yahia, Optical constants, photo-stability and photo-degradation of MB/PMMA thin films for UV sensors. *Optik* **127**, 4959–4963 (2016). <https://doi.org/10.1016/j.ijleo.2016.02.027>
 28. M. Kleemann, A. Suisalu, J. Kikas, Polymer film doped with a solvatochromic dye for humidity measurement. *Proc. SPIE* (2006). <https://doi.org/10.1117/12.639189>
 29. A.F. Mansour, M.G. El-Shaarawy, S.M. El-Bashir, M.K. El-Mansy, M. Hammam, Optical study of perylene dye doped poly(methyl methacrylate) as fluorescent solar collector. *Polym. Int.* **51**, 393–397 (2002). <https://doi.org/10.1002/pi.857>
 30. S.M. El-Bashir, I.S. Yahia, F. Al-Harbi, H. Elburaih, F. Al-Faifi, N.A. Aldosari, Improving photo-stability and efficiency of polymeric luminescent solar concentrators by PMMA/MgO nanohybrid coatings. *Int. J. Green Energy* **14**, 270–278 (2017). <https://doi.org/10.1080/15435075.2016.1233422>
 31. S. Salmani, E. Safari, M.H. Majles Ara, M.S. Zakerhamidi, Optical bistability of azo dye-doped PMMA polymer. *Opt. Mater.* **35**, 1619–1622 (2013). <https://doi.org/10.1016/j.optmat.2013.04.002>
 32. T. Deligeorgiev, A. Vasilev, S. Kaloyanova, J.J. Vaquero, Styryl dyes - synthesis and applications during the last 15 years. *Color Technol.* **126**, 55–80 (2010). <https://doi.org/10.1111/j.1478-4408.2010.00235.x>
 33. C. Schwechheimer, F. Rönicke, U. Schepers, H.-A. Wagenknecht, A new structure–activity relationship for cyanine dyes to improve photo-stability and fluorescence properties for live cell imaging. *Chem. Sci.* **9**, 6557–6563 (2018). <https://doi.org/10.1039/C8SC01574K>
 34. U.N. Yadav, H.S. Kumbhar, S.S. Deshpande, S.K. Sahoo, G.S. Shankarling, Photophysical and thermal properties of novel solid state fluorescent benzoxazole based styryl dyes from a DFT study. *RSC Adv.* **5**, 42971–42977 (2015). <https://doi.org/10.1039/c4ra12908c>
 35. A.S. Basaleh, S.M. Sheta, Manganese metal-organic framework: chemical stability, photoluminescence studies, and biosensing application. *J. Inorg. Organomet. Polym.* **31**, 1726–1737 (2021). <https://doi.org/10.1007/s10904-021-01888-4>
 36. J. Garcia-Amorós, S. Swaminathan, Y. Zhang, S. Nonell, F.M. Raymo, Optical writing and reading with a photoactivatable carbazole. *Phys. Chem. Chem. Phys.* **17**, 11140–11143 (2015). <https://doi.org/10.1039/C5CP01336D>
 37. M.-D. Damaceanu, C.-P. Constantin, Tuning the light emission of novel donor-acceptor phenoxazine dye-based materials towards the red spectral range. *Opt. Mater.* **78**, 160–171 (2018). <https://doi.org/10.1016/j.optmat.2018.02.015>
 38. P. Miluski, M. Kochanowicz, J. Zmojda, D. Dorosz, 1,4-Bis(2-methylstyryl)benzene doped PMMA fibre for blue range fluorescent applications. *Spectrochim. Acta Part A Mol. Biomol. Spectrosc.* **192**, 88–92 (2018). <https://doi.org/10.1016/j.saa.2017.11.010>
 39. F. Huo, H. Zhang, Z. Chen, L. Qiu, J. Liu, S. Bo et al., Novel nonlinear optical push–pull fluorene dyes chromophore as promising materials for telecommunications. *J. Mater. Sci. Mater. Electron.* **30**, 12180–12185 (2019). <https://doi.org/10.1007/s10854-019-01576-7>
 40. A. Upadhyay, K. Subramanian, Synthesis and opto-electrical properties of carbazole functionalized quinoline based conjugated oligomer for luminescent devices. *J. Photopolym. Sci. Technol.* **28**, 755–762 (2015)
 41. S.-L. Hsu, C.-M. Chen, K.-H. Wei, Carbazole-based conjugated polymers incorporating push/pull organic dyes: Synthesis, characterization, and photovoltaic applications. *J. Polym. Sci. Part A Polym. Chem.* **48**, 5126–5134 (2010). <https://doi.org/10.1002/pola.24311>
 42. O. Korychenska, D. Guzmán, À. Serra, X. Ramis, J.V. Grazulevicius, Fluorescent thiol-epoxy thermosets obtained from diglycidylether of bisphenol A and carbazole based diepoxy monomer. *React. Funct. Polym.* **116**, 107–113 (2017). <https://doi.org/10.1016/j.reactfunctpolym.2017.04.007>
 43. B.S. Singh, H.R. Lobo, G. Krishna Podagatlapalli, S. Venugopal Rao, G.S. Shankarling, Thiazole based novel functional colorants: synthesis, characterization and nonlinear optical studies using picosecond Z-scan technique. *Opt. Mater.* **35**, 962–967 (2013). <https://doi.org/10.1016/j.optmat.2012.11.018>
 44. M. Jachak, S. Khopkar, A. Chaturvedi, A. Joglekar, G. Shankarling, Synthesis of novel viscosity sensitive pyrrolo-quinoline based styryl dyes: photophysical properties, electrochemical and DFT study. *J. Photochem. Photobiol. A Chem.* **397**, 112557 (2020). <https://doi.org/10.1016/j.jphotochem.2020.112557>
 45. H. Kafafy, H. Wu, M. Peng, H. Hu, K. Yan, R.M. El-shishtawy et al., Steric and solvent effect in dye-sensitized solar cells utilizing phenothiazine-based dyes. *Int. J. Photoenergy* (2014). <https://doi.org/10.1155/2014/548914>
 46. A.K. Sanap, G.S. Shankarling, Environmentally benign synthesis of 4-aminoquinoline-2-ones using recyclable choline hydroxide. *New J. Chem.* **39**, 206–212 (2015). <https://doi.org/10.1039/C4NJ01281J>
 47. S.M. El-Bashir, A.A. Al-Jaghwan, Perylene-doped polycarbonate coatings for acrylic active greenhouse luminescent solar

- concentrator dryers. *Results Phys* **16**, 102920 (2020). <https://doi.org/10.1016/j.rinp.2019.102920>
48. X.M. Sang, X.J. Yang, Z.D. Cui, S.L. Zhu, J. Sheng, Preparation and characterization of nano-TiO₂ doped polystyrene materials by melt blending for inertial confinement fusion. *J. Macromol. Sci. Part B* **43**, 871–882 (2004). <https://doi.org/10.1081/MB-120030911>
49. M. Hamzah, S. Mezan, A. Tuama, A. Jabbar, M. Agam, Study and characterization of polystyrene/titanium dioxide nanocomposites (PS/TiO₂ NCs) for photocatalytic degradation application: a review. *Int. J. Eng. Technol.* **7**, 538–543 (2018)
50. J. Songkhao, R. Banerjee, S. Debnath, S. Narasimhan, N. Wannaprom, P. Vanalabhatana et al., Structure-property relationship of π -extended boron-dipyrromethene derivatives towards optoelectronic applications. *Dye Pigment* **142**, 558–571 (2017). <https://doi.org/10.1016/j.dyepig.2017.03.050>
51. A.M. Brouwer, Standards for photoluminescence quantum yield measurements in solution (IUPAC Technical Report). *Pure Appl. Chem.* **83**, 2213–2228 (2011). <https://doi.org/10.1351/pac-rep-10-09-31>
52. S. Khopkar, M. Jachak, G. Shankarling, Novel semisquaraines based on 2, 3, 3, 8-tetramethyl-3H-pyrrolo [2, 3- f] quinoline: Synthesis, photophysical properties, AIE, viscosity sensitivity and DFT study. *Dye Pigment* **161**, 1–15 (2019). <https://doi.org/10.1016/j.dyepig.2018.09.026>
53. J. Cazes (ed.), *Analytical Instrumentation Handbook*, 3rd edn. (CRC Press, Boca Raton, 2004). <https://doi.org/10.1201/9780849390395>
54. S.M. El-Bashir, M.S. AlSalhi, F. Al-Faifi, W.K. Alenazi, Spectral properties of PMMA films doped by perylene dyestuffs for photoselective greenhouse cladding applications. *Polymers* **11**, 494 (2019). <https://doi.org/10.3390/polym11030494>
55. M. Masili, L. Ventura, Equivalence between solar irradiance and solar simulators in aging tests of sunglasses. *Biomed. Eng. Online* **15**, 86 (2016). <https://doi.org/10.1186/s12938-016-0209-7>
56. S.C. Bhatia, 2—solar radiations, in *Bhatia SCBT-ARES* (Woodhead Publishing India, 2014), pp. 32–67. <https://doi.org/10.1016/B978-1-78242-269-3.50002-4>
57. A. Leszczyńska, J. Njuguna, K. Pielichowski, J.R. Banerjee, Polymer/montmorillonite nanocomposites with improved thermal properties: Part I. Factors influencing thermal stability and mechanisms of thermal stability improvement. *Thermochim. Acta* **453**, 75–96 (2007). <https://doi.org/10.1016/j.tca.2006.11.002>
58. B. Demirel, A. Yaraş, H. Elçiçek, Crystallization Behavior of PET Materials. *Bahkesir Üniversitesi Fen Bilim Enstitü Derg* **13**, 26–35 (2011)

Publisher's Note Springer Nature remains neutral with regard to jurisdictional claims in published maps and institutional affiliations.